LAWRENCE
LIVERMORE
NATIONAL
LABORATORY

UCRL-JRNL-212589

27Al and 1H Solid State NMR Studies Show Evidence of TiAl3 and TiH2 in Ti-doped NaAlH4

J. Herberg, R. Maxwell, E. Majzoub

May 27, 2005

Journal of alloysa and compounds

^{27}Al and ^{1}H Solid State NMR Studies Show Evidence of $TiAl_3$ and TiH_2 in Ti-doped $NaAlH_4$

Julie L. Herberg[1*], Robert S. Maxwell[1], Eric H. Majzoub[2]

[1] Lawrence Livermore National Laboratories, Livermore, CA, 94551 USA

[2] Sandia National Laboratories, Livermore, CA, 94551 USA

May 26, 2005

Abstract

Previous X-ray Diffraction (XRD) and Nuclear Magnetic Resonance (NMR) studies on Ti-doped $NaAlH_4$ revealed the reaction products of two heavily doped (33.3 ȧt. %) samples that were solvent-mixed and mechanically-milled. This investigation revealed that nano-crystalline or amorphous Al_2O_3 forms from the possible coordination of aluminum with oxygen atom of the furan ring system from added tetrahydrofuran (THF) in the solvent-mixed sample, and that $TiAl_3$ forms in mechanically-milled samples.[1] The present paper provides a more sophisticated NMR investigation of the these materials. On heavily doped (33.3 ȧt. %) solvent-mixed samples, ^{27}Al Magic Angle Spinning (MAS) NMR ^{27}Al multiple quantum MAS (MQMAS) indicates the presence of an oxide layer of Al_2O_3 on the surfaces of potentially bulk nanocrystalline Ti, nanocrystalline $TiAl_3$, and/or metallic aluminum. The ^{1}H MAS NMR data also indicate the possible

*Corresponding author. Tel.: +1-925-422-5900; *E-mail address:* herberg1@llnl.gov

coordination of aluminum with the oxygen atom in the THF. On heavily doped samples that were mechanically milled, ^{27}Al MAS NMR and static NMR confirms the presence of $TiAl_3$. In addition, the ^{1}H MAS NMR and ^{1}H spin-lattice relaxation (T_1) measurements are consistent with the presence of TiH_2. These results are in agreement with recent XAFS measurements indicating both Al and H within the first few coordination shells of Ti in the doped alanate.

Keywords: Hydrogen storage; Ti-doped $NaAlH_4$; ^{27}Al MAS NMR; ^{27}Al MQMAS NMR

1 Introduction

The development of Ti-doped sodium aluminum hydrides has gained attention because of its large weight percentage of hydrogen (5.5% ideal) compared to interstitual hydrides. The kinetics of the absorption and desorption of H_2 improves dramatically by the addition of transition metal dopants, in the form of Ti-halides such as $TiCl_3$.[1,2] However, the mechanism of enhanced kinetics due to the Ti-dopant in sodium aluminum hydride is still unknown.

Recently, we reported on Ti-doped sodium aluminum hydrides that were completely-reacted (33.3 ȧt. %-doped) with $TiCl_3$. These samples were processed in two different ways: one was solvent-mixed and the other was mechanically-milled.[1] The present paper explores the ^{27}Al and ^{1}H solid state NMR results of these fully-reacted samples in further detail. These reactions and the resultant products are crucial for understanding the conditions under which these materials can be most effectively doped for large scale applications. The ease of solution doping over mechanical milling is clear, however, the products of the doping

process in THF, as presented in this paper, suggest that other solvents may be more suitable for large scale production.

NMR can provide detailed understanding of the influences of metal incorporation on structure, composition, formation kinetics, hydrogen speciation, modes of hydrogen interaction, and release and reversibility mechanisms. It is therefore an ideal method to examine sodium alanate materials. Tarasov et al[3,4] have performed ^{23}Na and ^{27}Al NMR on $NaAlH_4$ and $NaAlD_4$ materials and have seen dramatic changes in the composition of these materials with various temperatures. The ^{23}Na static NMR data shows a line narrowing at -3 ppm with a linewidth of 250 Hz at a temperature of 178^{o}C. The authors attribute this line narrowing to the mobile Na^+ ion in $NaAlD_4$. While at temperatures in the range of 490-600°C, ^{23}Na static NMR data shows a broad signal with second-order quadrupolar splitting, which corresponds to NaD lineshapes. In the ^{27}Al static NMR data from these authors, they saw three main peaks that they attributed to Na_3AlD_6, aluminum metal, and $NaAlD_4$. They found that the Na_3AlD_6 species were most stable around 210-220°C, the aluminum metal species increased with temperature, and $NaAlD_4$ species were most stable around 180-200°C.

Doping $NaAlH_4$ with $Ti(OC_4H_9^n)_4$ in tolune, Bogdanovic et al.[2] went one step further in exploring the effects that Ti-doping has on the dehydrogenation and rehydrogenation cycles by performing ^{23}Na and ^{27}Al MAS NMR this material, confirming the transformation to hexahydride and bulk aluminum during decomposition, and further showing the incomplete re-hydrogenation step. Although they were unable to determine how Ti-doping affects this material, the authors show that the addition of Ti catalyst leads to a shoulder on the right side of one of the main Al X-ray diffraction peaks and tenatively assign this peak to an Al-Ti alloy.

Further solid state NMR studies have been performed on similar materials, such as Ti-

doped $LiAlH_4$. Balema et al.[5] and Wiench et al.[6] provide a detailed analysis of this material after it was mechanically-milled. These authors examined the thermal decomposition using high-temperature solid state ^{27}Al NMR. From XRD analysis, they determined that the high catalytic activity of $TiCl_3$ occurs because of the formation of microcrystalline $TiAl_3$.

In this paper, we performed ^{27}Al MAS NMR, ^{27}Al MQ MAS NMR, ^{1}H MAS NMR, and ^{1}H spin-lattice relaxation measurements (T_1) on fully-reacted samples that were either dissolved in THF or mechanically-milled. THF is known to coordinate strongly with transition metals in solution, and we show that this results in the formation of Al_2O_3 in heavily doped samples. Our results indicate that Al and H coordinate with the Ti in solution mixed samples, in agreement with recent XAFS studies on lightly doped (a few at. %) $NaAlH_4$.[7]

2 Experimental Details

2.1 Sample preparation

The samples prepared for this work are listed in Table (1). Millimeter sized crystals of $NaAlH_4$ were grown by solvent evaporation from *Sigma Aldrich* 1 M solutions of $NaAlH_4$ in THF, with $TiCl_3$ added to the solution at 4 at. %, with respect to the amount of alanate in solution, before the solvent evaporation. The single crystal samples were subsequently crushed in a mortar and pestle for diffraction and NMR analysis. All samples were prepared in an argon glove box. These samples are referred to as (S_2). Rapidly dried 4 at. % doped samples, prepared in THF, resulted in fine powders and are referred to as (S_3). Some samples of (S_3) were also mechanically milled, and are referred to as (S_4). A further explanation of these samples is discussed elsewhere.[1]

2.2 NMR Measurements

MAS NMR measurements were performed on a Bruker Avance 400WB spectrometer with a magnetic field of 9.4 T. This gives a resonance frequency of 104.25 MHz for ^{27}Al (spin $\frac{5}{2}$) and 400.13 MHz for ^{1}H (spin $\frac{1}{2}$). The samples were packed in 4 mm MAS rotors inside an Ar glove box with oxygen levels below 3 ppm. Spinning rates of 9 kHz and 12 kHz were used. The Free Induction Decay (FID) spectra were taken with a single excitation pulse. For ^{27}Al, a short pulse of 8 degree flip angle of 0.2 μs was used. ^{1}H MAS NMR was taken with a 90 degree pulse width of 4.2 μs. The ^{27}Al spectra were referenced to 0.1M aqueous solutions of $Al(NO_3)_3$ ar 0ppm and the ^{1}H NMR spectra were referenced to tetramethylsilane (TMS) at 0ppm.

The ^{1}H NMR spin-lattice relaxation times (T_1) were measured using a saturation-recovery method, as described by Fukushima.[8] The inspection of the partially recovered longitudinal magnatization was performed by using $\pi/2$(x)-τ-$\pi/2$(y) echo. The T_1 times were determined by fitting $M(\tau)/M_o$ to a multi-exponential growth curve: ($M(\tau)/M_o = \sum_{i=1}^{inf} X_i$(1-exp(-$\tau/T_1$)).[8]

^{27}Al MAS NMR resonances are typically broadened by non-negligible second order anisotropic effects.[9] Recent experimental methods, however, have been developed utilizing a combination of MAS and Multiple Quantum evolution which serve to provide high resolution spectra of I=5/2 spins.[10] For the ^{27}Al Multiple Quantum MAS (3QMAS) experiments, a standard two pulse z-filtered pulse sequence was used.[11] The non-selective 148 kHz $\pi/2$ pulse length was 1.75 μs at the power levels used. The conversion pulse was optimized at 2.5 μs and the reconversion pulse optimized to 0.8 μs. The z-filter pulse was 20 μs after the reconversion pulse and was set to 50 μs with 30 dB of additional attenuation on the RF power level. Data

was acquired and processed using the states method and the data was shear transformed in the indirect dimension according to Massiot, et al.[11,12] The resonance frequency was set to the frequency of $Al(H_20)^{3+}$ (0ppm). The quadrupolar coupling parameters, which include second order quadrupolar effects (SOQE = $C_Q(1+\eta^2/3)^{1/2}$, where C_Q is the quadrupolar coupling constant and η is the asymmetry parameter) and isotropic chemical shifts (δ_{iso}) have been estimated from analysis of the resonance position in the unsheared spectra.[13] C_Q and η were then estimated by fitting the anisotropic line shapes with the DMFIT program.[14]

3 Results and Discussion

As we previously reported, the Rietveld refinement using powder X-ray diffraction of 4 at. % Ti-doped $NaAlH_4$ shows no observable shift in the lattice constants due to the exposure of Ti, indicating that the Ti does not enter the bulk of the $NaAlH_4$ lattice.[1] A large dopant level was used (33 at. %) in order to fully react the $NaAlH_4$ and yield large amounts of reaction products. These fully-reacted samples would theoretically result in the formation of NaCl, $TiAl_3$, and/or TiH_2, and bulk Al.[1]

The fully-reacted (33 at. %-doped) sample that was solvent-mixed with THF (S_4) showed no evidence of bulk Ti or $TiAl_3$ in X-ray diffraction. Further, ^{23}Na MAS NMR studies on this same material confirmed that all of the ^{23}Na in this sample was in the form of NaCl, indicating that the sample was fully-reacted.[1] The ^{27}Al MAS spectrum is shown in Figure (1). The ^{27}Al MAS spectrum for this sample shows a peak at 1641 ppm, which represents metallic aluminum, and three overlapping peaks at 8.4 ppm, 35.5 ppm, and 63.6 ppm, which represents six, five, and four coordinate aluminum-oxygen species.[15] To determine that the three overlapping peaks did not represent AlH_4 species, ^{27}Al $\{^1H\}$ MAS NMR was performed. If

AlH_4 species were responsible for these resonances, the resulting ^{27}Al NMR spectra would be expected to be broadened significantly due to large Al-H dipole-dipole couplings. This broadening, however, should be removed upon the application of ^{1}H decoupling during acquisition. In the samples studies here no significant narrowing occurred upon decoupling in the ^{27}Al NMR spectra, strongly indicating that these resonances are due to Al_2O_3 peaks and not to AlH_4.

To gain further insight into the speciation of the ^{27}Al peaks observed in the 0-100 ppm range, we performed a ^{27}Al MQMAS experiment on this sample. The sheared ^{27}Al MQMAS data is shown in Figure (2) with the horizontal axis representing the anisotropic dimension and the vertical axis representing the isotropic dimension. Three isotropic resonances were observed with broad anisotropic projections shown in the inset. The 2D lineshapes were not observed to smear as expected when distributions of chemical shift anisotropies of quadupolar coupling exist.[16] The anisotropic projections are all parallel with the horizontal axis and are consistent, within the uncertainty determined by the moderate signal-to-noise, with second order dominated MAS spectra without large distributions of chemical shifts or quadrupole coupling constants. Increased signal to noise spectra were not possible given the reactive nature of these samples with oxygen.

The quadrupolar coupling parameters, which include SOQE, δ_{iso}, C_Q, and η, have been estimated from analysis of the resonance position in the unsheared spectra and fitting in the projections in frequency are shown in Table (2).[13] The quadrupolar coupling parameters are in agreement with other reported values for Al_2O_3.[16,17]

From the anisotropic chemical shifts and these coupling parameters, we have assigned the resonances in the 100-0 ppm range to 1) octahedral (0 to 10 ppm), 2) pentacoordinate (around 30 ppm), and 3) tetrahedral (40 to 80 ppm) Al-oxide sites.[15] The quadrupolar coupling con-

stants and the fact that there exists no smearing in the ^{27}Al MQMAS data indicate that this system is rather ordered in nature. However, the X-ray Diffraction data shows no evidence of crystalline Al_2O_3. In the X-ray Diffraction data there is evidence of an extremely broad peak that could be attributed to material with a coherence length about 7-10 Å, which is mostly likely due to nanocrystalline Ti and/or $AlTi_3$. Even though the form of the nanocrystalline titanium is unknown, the picture of Ti, $AlTi_3$, and/or metallic aluminum in the bulk with a surrounding layer of amorphous Al_2O_3 on the surface is consistent with the ^{27}Al MQMAS NMR data. This would mean that the rather sharp peaks in the ^{27}Al MQMAS data of the different Al_2O_3 species represent amorphous Al_2O_3. On similar materials, others[18,19] have found that the presence of pentacoordinate Al_2O_3 in ^{27}Al MQMAS data possibly represents amorphous Al_2O_3, rather than crystalline Al_2O_3.[19] This conclusion is still widely debated. However, in this case, both the X-ray Diffraction data and the sharp, isotropic peaks of the different forms of Al_2O_3 in the ^{27}Al MQMAS NMR spectrum on the solvent-mixed sample strongly indicate that the ^{27}Al NMR signal arises from nano-crystalline Al_2O_3. The presence of Al_2O_3 in this sample (S_4) indicates the presence of oxygen, which could either come from contamination of the sample during processing, dissociation of THF to produce oxygen that are attached to the aluminum in the form of Al_2O_3, or the coordination of the oxygen atom on the furan ring in THF resulting in a reorientation of the aluminum atoms with the oxygen atom to form Al_2O_3.

Contamination seems unlikely. If contamination occurred, then one would expect to see the same type of contamination in the sample that was ball-milled (S_5) because the authors were careful to treat both these samples in the exact same manner. In the ^{1}H NMR spectra of sample S_5, there is no evidence of contamination in this sample. This is discussed further in a later section of this paper.

As for the second possibility, THF is one of the most polar ethers and is extremely soluble in water. It is not considered to be readily degradable. For this reason, THF is used as a solvent for polar reagents. However, THF has been known to decompose when exposed to a catalyst, such as organolithiums.[20] Thus, it is not out of the question that this might occur. The possible decomposition products of THF would be CH_2 and OH groups, but to speculate on the ^{1}H NMR chemical shift of these signatures in the presence of titanium is rather difficult and beyond the scope of this paper. We also attempted to perform ^{13}C NMR on this sample, but we were unable to obtain a signal because there only exists a small amount of carbon in this system. The most likely senario of the origin of the oxygen in Al_2O_3 would be the coordination of aluminum on internal surfaces of the metallic aluminum coordinated with oxygen atoms of the heteroatomic furan ring in THF. This same senario has been seen in other metal systems, including aluminum, lithium, and magnesium, where the strong ionic metal-oxygen bond can lead to an sp^2-type lone pair orbital, which can act as a dative bond to a metal center.[21,22] This possiblity was also predicted by Fichtner et al.[23] From the ^{1}H MAS NMR data, which is shown in Figure (3), the origin of the oxygen in the Al_2O_3 cannot be fully determined. However, the ^{1}H MAS NMR data can provide insight into the structure of the protons in sample S_4 that was solvent mixed. THF typically gives signal at 1.72 ppm and 3.58 ppm for ^{1}H MAS NMR spectra.[24] From the ^{1}H MAS NMR spectrum on sample (S_4), the ^{1}H MAS NMR peaks occur at 1.7 ppm, 4.8 ppm, and 8.7 ppm. From a paper examining how THF impacts clathrate hydrates for hydrogen storage, Lee et al.[25] found that they could distinguish between H_2O, H_2 in small cages, H_2 in large cages, and THF through both ^{1}H MAS NMR and Raman Scattering. By comparing these authors' ^{1}H MAS NMR results with our results, we can conclude that ^{1}H NMR peak at 1.7 ppm represents aliphatic protons in the THF that are weakly interacting with the oxygen in THF, the ^{1}H NMR peak

at 4.8 ppm represents H_2 in small cages in interstitual sites, and ^{1}H NMR peak at 8.2 ppm most likely represents H_2O. The question here is what happens to the ^{1}H NMR THF peak at 3.58 ppm, which represents the aliphatic protons in the THF that are strongly interacting with the oxygen in THF. The possible explanation for this location of the ^{1}H NMR THF peak at 3.58 ppm is that it is embedded in the wide linewidth of the ^{1}H MAS NMR peak at 4.8 ppm. If the oxygen from THF is coordinated with the aluminum to form Al_2O_3, then one would expect the ^{1}H NMR THF peak at 3.58 ppm to be slightly shifted, but within the wide linewidth of the ^{1}H MAS NMR peak at 4.8 ppm. This makes the scenario of the origin of the oxygen in Al_2O_3 that would occur from the coordination of aluminum on surfaces of the metallic aluminum coordinated with oxygen atoms in THF highly probable.

Even though both XRD and NMR showed no evidence of $TiAl_3$ in the sample S_5, and only the presence of metallic aluminum and Al_2O_3, the ^{27}Al MAS NMR data on the mechanically-milled sample (S_5) did show evidence of $TiAl_3$, as shown in Figure (4a). There are four resonance: two at approximately 10 ppm and 103 ppm, with respective linewidths of 19 ppm and 30 ppm, a broad resonance at approximately 664 ppm, and a small amount of metallic aluminum at 1640 ppm. Our previous studies compared this signal with a sample of pure $TiAl_3$ in the $L1_2$ metabstable structure. This suggested the existance of $TiAl_3$ in the mechanically-milled sample (S_5).[1] As indicated by others investigating similar materials,[6] a full understanding of the aluminum species in this material is not straight forward. The metallic aluminum signal in the ^{27}Al MAS NMR data on sample (S_5) occurs at 1640 ppm, which is extremely small integrated intensity due to the excitation bandwidth limitations. Most likely, this sample has only a small amount of metallic aluminum. Balema et al.[5] have found that $TiAl_3$ is present in mechanically-milled Ti-doped $LiAlH_4$. Through XRD and ^{27}Al NMR, these authors showed that the ball-milling process leads to transformation

of the $TiAl_3$ from a DO_{22} phase into a metastable phase $L1_2$. Quadrupolar interactions, Knight shifts, and spin-lattice relaxation times in $TiAl_3$ can provide information about site occupation and Fermi-surface effects. Since quadrupolar and anisotropic Knight shift effects typically complicates the central transition ($\frac{1}{2} \rightarrow$-$\frac{1}{2}$), the satellite transitions that are due to quadrupolar broadening from high order transitions can provide further insight into this material. From Figure (4) b), which is a ^{27}Al static NMR spectrum of sample S_5; it is apparent that some satellite transitions are present, but to gather further information from this spectrum would be difficult due to the poor signal-to-noise. However, the observed $TiAl_3$ is paramagnetically shifted, which means that paramagetic shielding adds to the overall magnetic field experienced by the nucleus. This is similar to other static ^{27}Al NMR data.[26]

While $TiAl_3$ is present in the fully-reacted mechanically milled sample (S_5), the location of the residual hydrogen in this material (indicated by ^{1}H NMR) is still unknown. For this sample (S_5), the ^{1}H MAS NMR lineshape is shown in Figure (5) is extremely broad. From other studies on Ti-Al-H alloys,[27] it has been shown that hydrogen in the form of TiH_2 produces a broad ^{1}H NMR lineshape. These authors also showed that samples that were contaminated with oxygen and carbon produced a narrow ^{1}H NMR lineshape superimposed on a broad ^{1}H NMR lineshape. Therefore, the broad nature of the ^{1} NMR lineshape of sample S_5 is consistent with the presence of TiH_2. The ^{1}H NMR spin-lattice relaxation (T_1) measurements of samples S_2, S_3, S_4, and S_5 are shown in Figure (6). In sample (S_2), which is likely pure $NaAlH_4$, there is only one long T_1 relaxation process. Sample (S_3) also shows only one T_1 relaxation process. However, in samples (S_4) and (S_5) there is likely more than one relaxation process, perhaps indicating that there are three different local environments for the fully-reacted samples. The T_1 values are shown in Table (3). These results are similar to Korn et al.,[27] who showed through ^{1}H T_1 NMR measurements that hydrogen in

a Ti-Al-H system has at least three different crystallographic environments with different diffusion characteristics. Korn et al. found that one of the T_1 processes would likely be due to TiH_2, which would possess a fast T_1 relaxation rate, since the hydrogen is in contact with the titanium. In fact, Korn et al. indicate a T_1 relaxation time for TiH_2 in the presence of 16.3 åt. %of aluminum to be approximately 30-40 ms at room temperature, which is close to the fast T_1 relaxation time of 40. 1ms for S_5. Thus, this fast T_1 relaxation process clearly exists in samples (S_4) and (S_5), but the different hydrogen processes can be distinguished by their different relaxation times. Both the fully-reacted sample that was solvent-mixed (S_4) and the mechanically-milled sample (S_5) has one very fast relaxing ^{1}H NMR T_1 process. Since these samples were fully reacted, the possibility of the existence of Ti-H-Al is rather unlikely, while the existence of TiH_2 is likely to exist in these samples.

4 Conclusions

Our ^{27}Al MQMAS experiments indicate that fully-reacted THF solvent-mixed samples contain an oxide layer of Al_2O_3, potentially around bulk nanocrystalline Ti, nanocrystalline $TiAl_3$, and/or metallic aluminum. Examination of the ^{1}H MAS NMR data from this sample suggests that the source of oxygen in Al_2O_3 was likely due to the THF molecule being coordinated with aluminum in a Ti-Al compound or nanocluster. These results clearly indicate the extremely different compounds which may result in solvent mixed samples, as opposed to mechanically milled samples, where the ^{27}Al MAS and static NMR studies show the presence of $TiAl_3$. Finally, the ^{1}H MAS NMR and ^{1}H spin-lattice relaxation measurements (T_1) indicate the presence of TiH_2 in fully-reacted mechanically milled sample.[28,29]

Acknowledgements

The authors would like to thank Dr. Robert Bowman, Dr. Sarah C. Chinn, and Dr. Julie Perkins for their insights. This work was funded by the U.S. Department of Energy, Office of Energy Efficiency and Renewable Energy, in the Hydrogen, Fuel Cells & Infrastructure Technologies Program under contract No. DE-AC36-83CH10093, and Sandia National Laboratories through the Laboratory Directed Research and Development program. NMR work was performed under the auspices of the U.S. Department of Energy by University of California, Lawrence Livermore National Laboratory under Contract W-7405-Eng-48.

Figure Captions

Figure 1: ^{27}Al MAS NMR spectra of $3NaAlH_4$ + $TiCl_3$ that was solution-mixed with THF (S_4). The data was taken with a 8 degree pulse width of 0.2μs and spinning at 12kHz.

Figure 2: The ^{27}Al MQMAS data was taken with a spinning speed of 12kHz on sample S_4. The sheared ^{27}Al MQMAS data is a two-dimensional fourier transform plot of a triple/single-quantum correlation to highlight the isotropic and anisotropic nature of the ^{27}Al nuclei in this material. In this plot, the horizontal dimension represents single quantum coherence or isotropic and anisotropic coherence. The verticle dimension represents multiple quantum dimension and only contains information about isotropic coherences. The quadrupolar shifts for each peak are also presented.

Figure 3: ^{1}H MAS NMR spectra of $3NaAlH_4$ + $TiCl_3$ that was solution-mixed with THF (S_4). The data was taken with a spinning at 12kHz. * indicates an offset signal.

Figure 4: ^{27} MAS NMR spectra of $3NaAlH_4$ + $TiCl_3$ that was mecannically-milled (S_5). The data was taken with a 8 degree pulse width of 0.2μs. a) spinning at 12kHz b) static.

Figure 5: ^{1}H MAS NMR spectra of $3NaAlH_4$ + $TiCl_3$ that was mechanically milled(S_5). The data was taken with a spinning at speeds of 12kHz. * indicates an offset signal

Figure 6:: ^{1}H spin-lattice relaxation measurements (T_1) of sample S_2, S_3, S_4, and S_5.

Table Captions

Table 1: Samples used in this work.

Table 2: The quadrupolar coupling parameters, which include second order quadrupolar effects (SOQE = $C_Q(1+\eta^2/3)^{1/2}$, where C_Q is the quadrupolar coupling constant and η is the asymmetry parameter) and isotropic chemical shifts (δ_{iso}) for the Al_2O_3 species determined from the unsheared ^{27}Al 3QMAS NMR spectra.

Table 3: The ^1H NMR spin-lattice relaxation (T_1) times for $NaAlH_4$ Ti-doped in different processes.

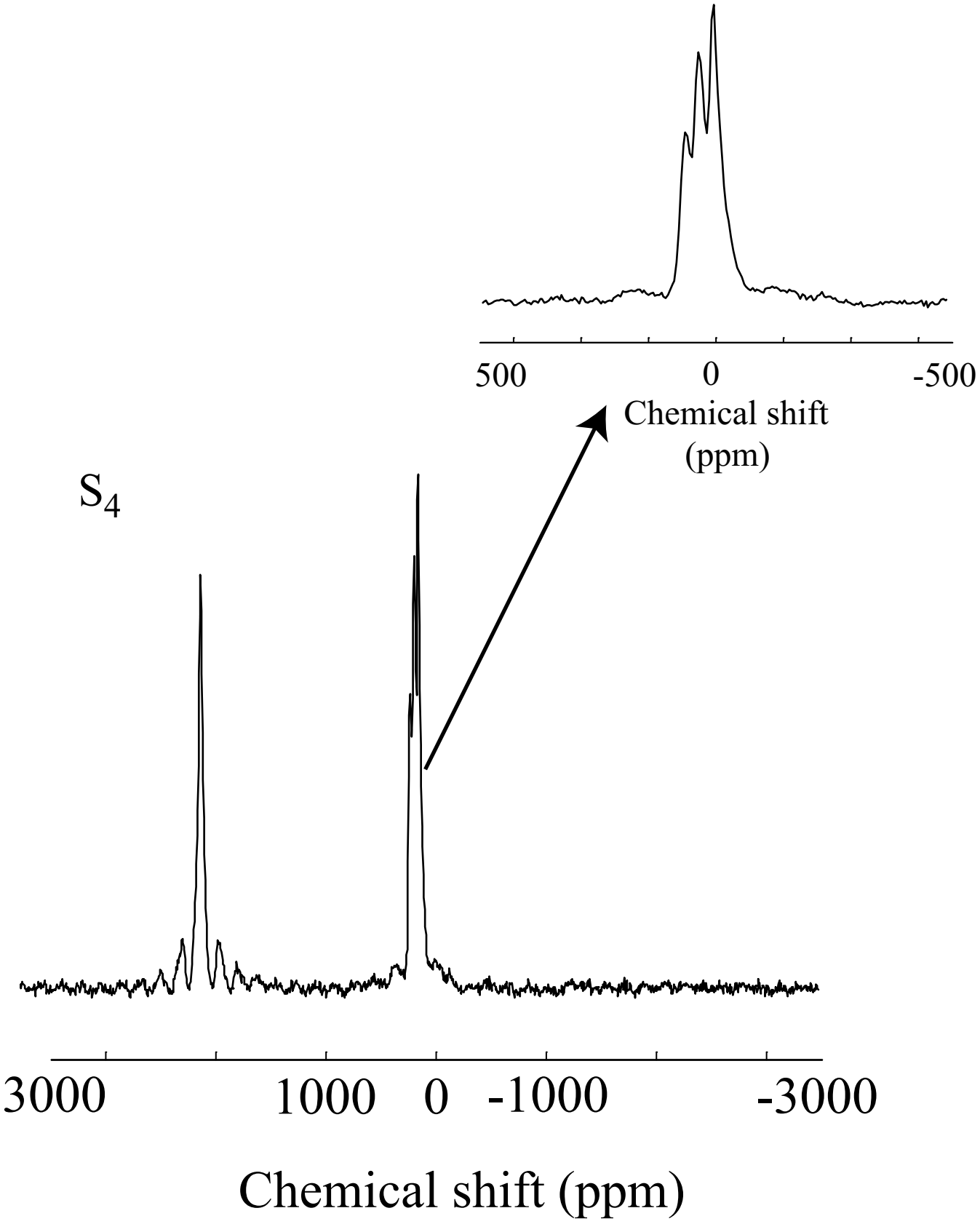
500
0
-500
Chemical shift
(ppm)
S4
3000
1000
0
-1000
-3000
Chemical shift (ppm)

Figure 1:

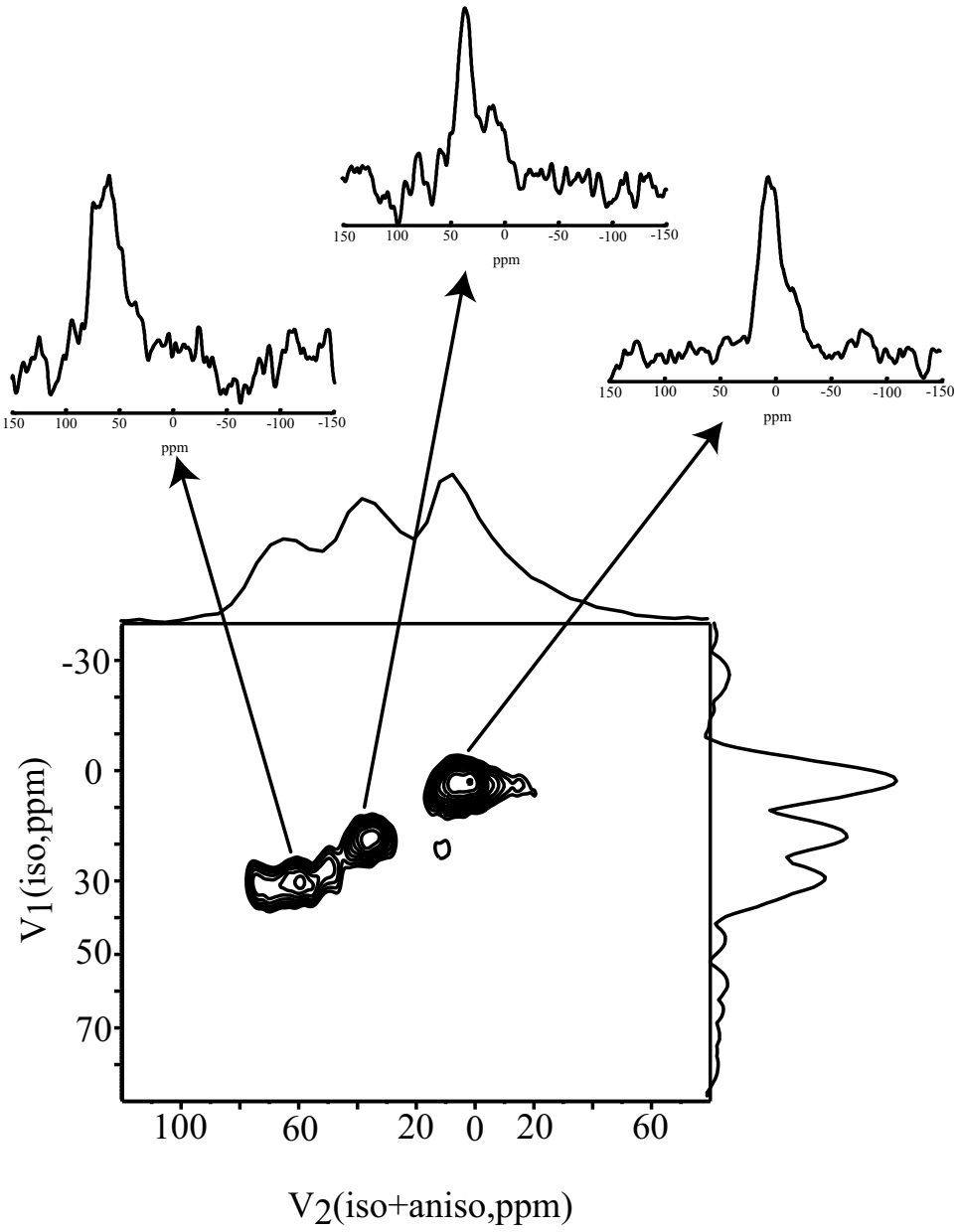
150 100 50 0 -50 -100 -150
ppm
150 100 50 0 -50 -100 -150
ppm
150 100 50 0 -50 -100 -150
ppm
-30
0
30
50
70
V1(iso,ppm)
100 60 20 0 20 60
V2(iso+aniso,ppm)

Figure 2:

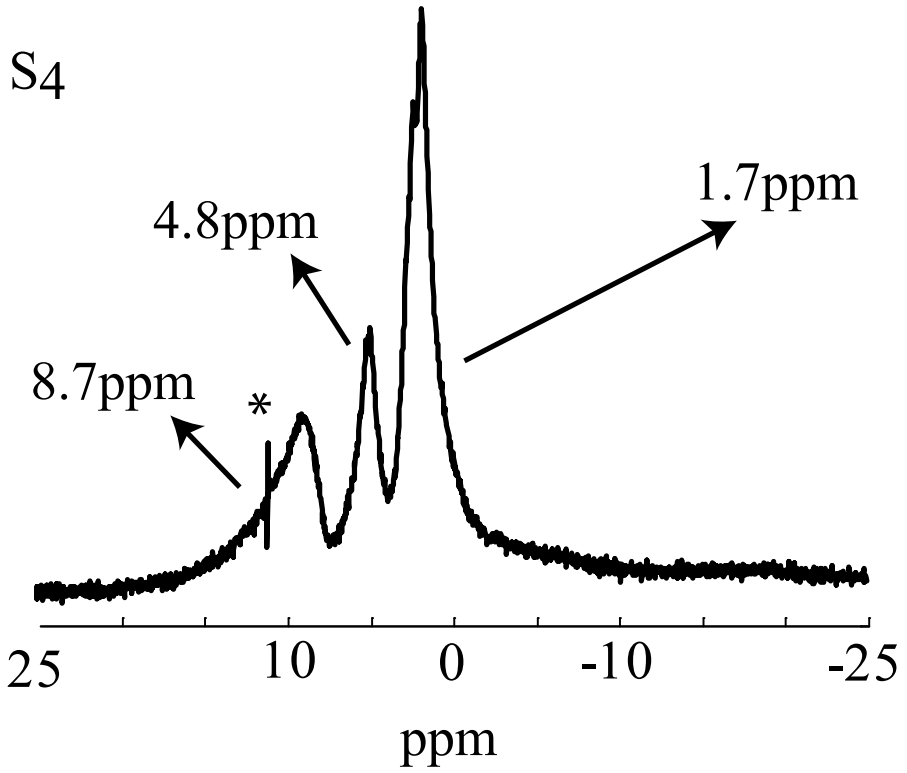

Figure 3:

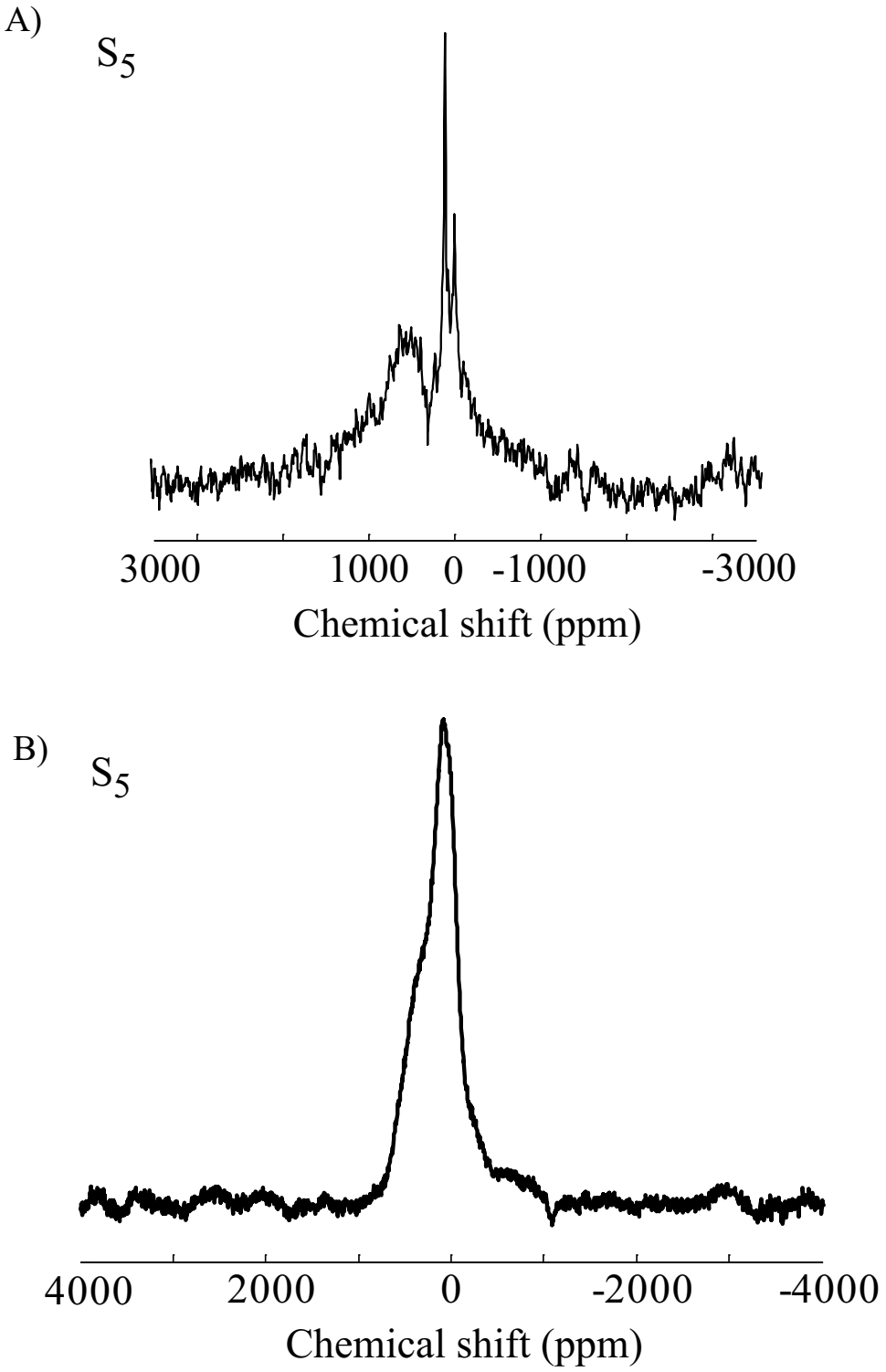
A)
S_5
3000
1000
0
-1000
-3000
Chemical shift (ppm)
B)
S_5
4000
2000
0
-2000
-4000
Chemical shift (ppm)

Figure 4:

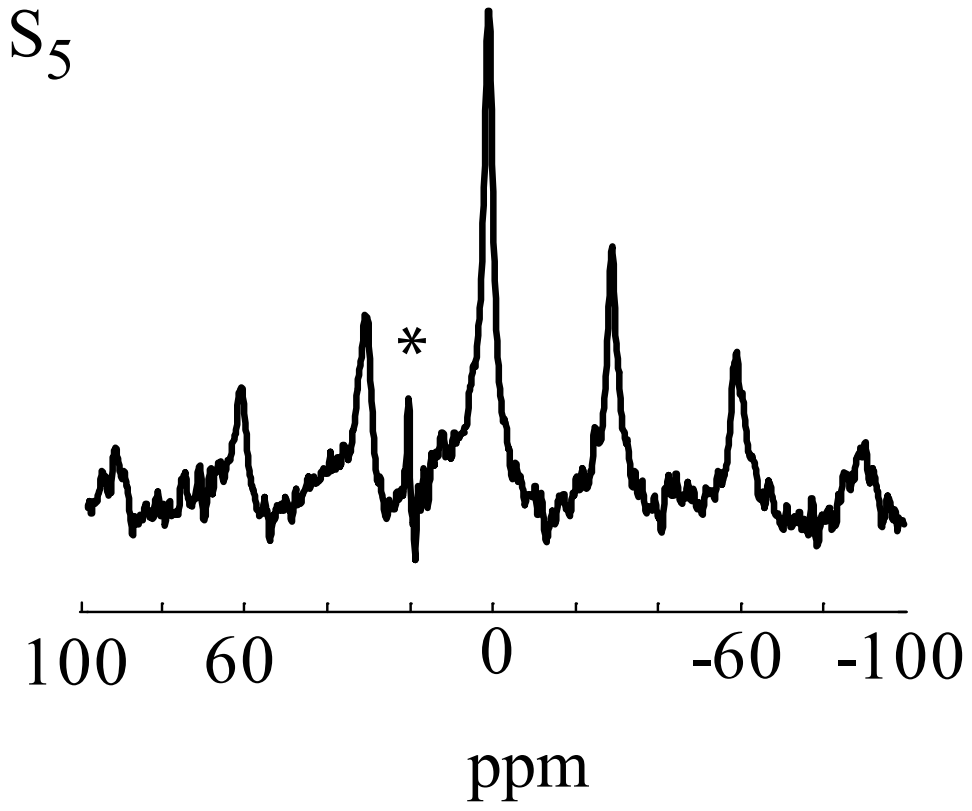

Figure 5:

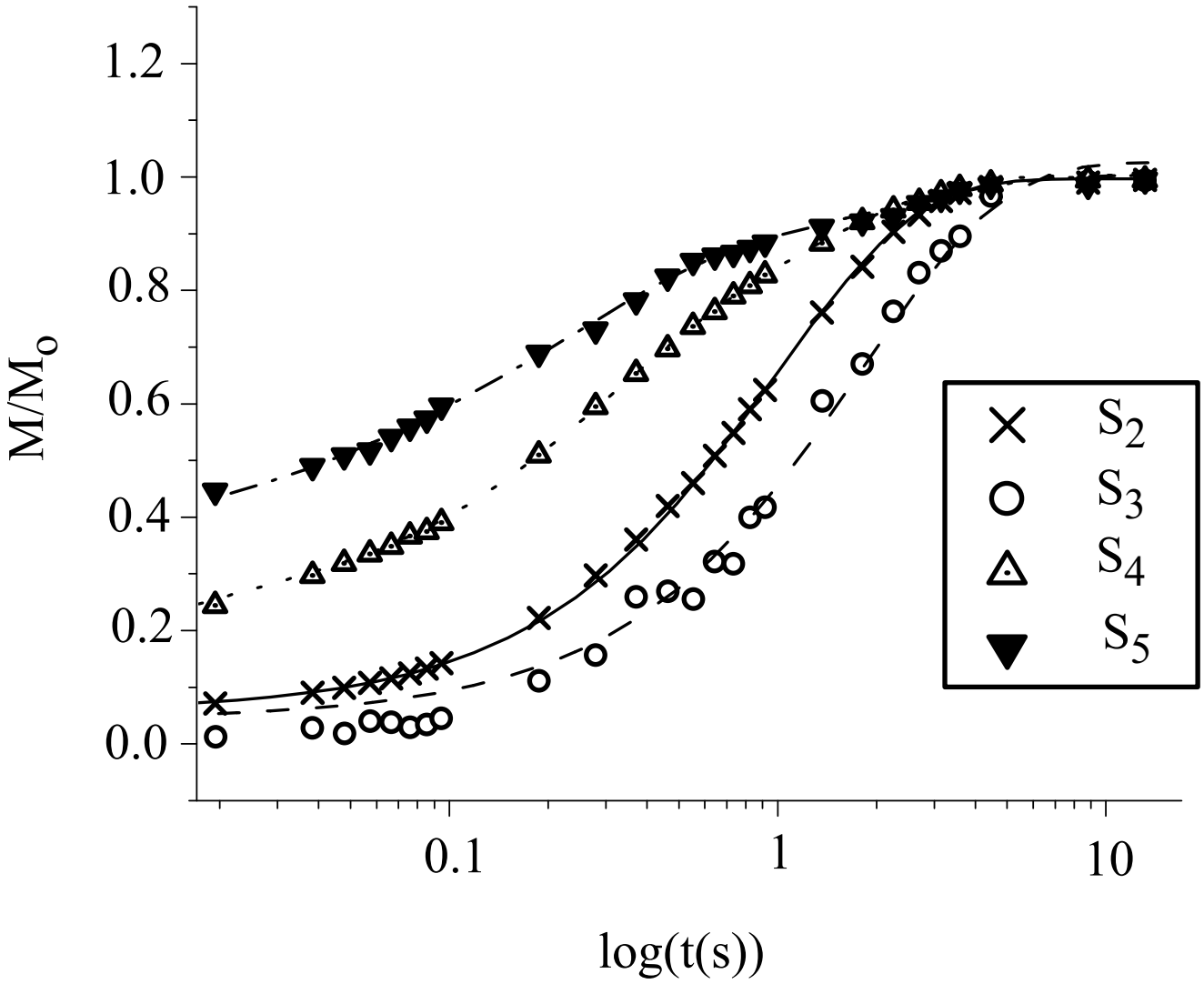

Figure 6:

Sample	Solution	Ti-precursor	at. % dopant	Form	Milled
S_2	THF	$TiCl_3$	4	crushed crystal	no
S_3	THF	$TiCl_3$	4	fine powder	no
S_4	THF	$TiCl_3$	33	fine powder	no
S_5	none	$TiCl_3$	33	fine powder	yes

Table 1:

Species	Chemical Shift(ppm)	SOQE(MHz)	δ_{iso}(ppm)	C_Q(Mhz)	η
Al_2O_3(four-fold)	8.4	5.0	9.4	4.9	0.33
Al_2O_3(five-fold)	35.5	7.6	35.1	7.5	0.20
Al_2O_3(six-fold)	63.6	7.1	66	6.8	0.52

Table 2:

Sample	S_2	S_3	S_4	S_5
$T_{1(1)}$	1.036s	1.935s	1.3036s	2.257s
$T_{1(2)}$			0.246s	0.246s
$T_{1(3)}$			0.009s	0.0401s

Table 3:

References

1. Majzoub, E. H.; Herberg, J. L.; Stumpf, R.; Maxwell, R. S. *Journal of Alloys and Compounds* **2004,** *394,*.

2. Bogdanovic, B.; Felderhoff, M.; Germann, M.; Hartel, M.; Pommerin, A.; Schuth, F.; Weidenthaler, C.; Zibrowius, B. *Journal of Alloys and Compounds* **2003,** *350,* 246-255.

3. Tarasov, V. P.; Bakum, S. I.; Privalov, V. I.; Muraviev, Y. B.; Samoilenko, A. A. *Physical Methods of Investigation* **1995,** *41,* 1104-1107.

4. Tarasov, V. P.; Kirakosyan, G. A. *Physical Methods of invesitgation* **1996,** *42,* 1223-1227.

5. Balema, V. P.; Wiench, J. W.; Dennis, K. W.; Pruski, M.; Pecharsky, V. K. *Journal of Alloys and Compounds* **2001,** *329,* 108-114.

6. Weinch, J. W.; Balema, V. P.; Pecharsky, V. K.; Pruski, M. *Journal of Solid State Chemistry* **2004,** *177,* 648-653.

7. Graetz, J.; Reilly, J. J.; Johnson, J.; Ignatov, A. Y.; Tyson, T. A. *Applied Physics Letters* **2004,** *85,* 500.

8. Fukushima, E.; Roeder, S. B. W. Addison-Wesley Publishing Company, Inc.: 1981.

9. Slichter, C. P. *Principles of Nuclear Magnetic Resonance;* Springer-Verlag: 1990.

10. Medek, A.; Harwood, J. S.; Frydman, L. *J. Am. Chem. Soc.* **1995,** *117,* 12779-12787.

11. Ganapathy, S.; Das, T. K.; Vetrivel, R.; Ray, S. S.; Sen, T.; Sivasanker, S.; Delevoye, L.; Fernandez, C.; Amoureux., J. P. *Journal of the American Chemical Society* **1998,** *120,* 4752-4762.

12. Massiot, D.; Touzo, B.; Trumeau, D.; Coutures, J. P.; Virlet, J.; Florian, P.; Grandinetti, P. J. *Solid State Nuclear Magnetic Resonance* **1996,** *6,* 73-83.

13. Fernandez, C.; Amoureux, J. P.; Chezeau, J. M.; Delmotte, L.; Kessler, H. *Microporous Materials* **1996,** *6,* 331-340.

14. Massiot, D.; Fayon, F.; Capron, M.; King, I.; Calve, S. L.; Alonso, B.; Durand, J.-O.; Bujoli, B.; Gan, Z.; Hoatson, G. *Magnetic Resonance in Chemistry* **2002,** *40,* 70-76.

15. Brinker, C. J.; Scherer, G. W. Academic Press: 1989.

16. Goldbourt, A.; Vega, S. *Journal of Magnetic Resonance* **2002,** *154,* 280-286.

17. Kraus, H.; Prins, R.; Kentgens, A. P. M. *J. Phys. Chem.* **1996,** *100,* 16336-16345.

18. Florian, P.; Gervais, M.; Douy, A.; Massiot, D.; Coutures, J. P. *J. Phys. Chem. B.* **2001,** *105,* 379-391.

19. McManus, J.; Ashbrook, S. E.; MacKenzie, K. J. D.; Wimperis, S. *Journal of Non-Crystalline Solids* **2000,** *282,* 278-290.

20. Clayden, J.; Yasin, S. A. *New. J. Chem.* **2002,** *26,* 191-192.

21. Sachdev, H.; Wagner, C.; Preis, C.; Huch, V.; Veith, M. *J. Chem. Soc. Dalton Trans.* **2002,** 4709-4713.

22. Gun'ko, Y.; Reilly, R.; Kessler, V. *New J. Chem.* **2001,** *25,* 528-530.

23. Fichtner, M.; Fuhr, O.; Kircher, O.; Rothe, J. *Nanotechnology* **2003,** *14,* 778-785.

24. Deng, F.; Hu, J.; Xiong, J.; Du, Y. *Solid State Nuclear Magnetic Resonance* **2003,** *2,* 97-103.

25. Lee, H.; Lee, J.; Kim, D.; Park, J.; Seo, Y.; Zeng, H.; Moudrakovski, I.; Ratcliffe, C. I.; Ripmeester, J. *Nature* **2005,** *434,* 743-746.

26. Lue, C.; Chepin, S.; Chepin, J.; Ross, J. H. *Physical Review B* **1998,** *57,* 33.

27. Korn, C.; Zamir, D.; Hadari, Z. *Acta Metallurgica* **1974,** *22,* 33-46.

28. Bastow, T. J.; Forwood, C. T.; Gibson, M. A.; Smith, M. E. *Physical Review B* **1998,** *58,* 2988.

29. Maeland, M. A.; Hauback, B.; Fjellvag, H.; Sorby, M. *International Journal of Hydrogen Energy* **1999,** *24,* 163-168.